Expanded functions for a family of plant intracellular immune receptors beyond specific recognition of pathogen effectors

Vera Bonardi[a], Saijun Tang[b], Anna Stallmann[a], Melinda Roberts[a], Karen Cherkis[c], and Jeffery L. Dangl[a,c,d,e,f,1]

[a]Department of Biology, [d]Howard Hughes Medical Institute, [c]Curriculum in Genetics and Molecular Biology, [e]Department of Microbiology and Immunology, and [f]Carolina Center for Genome Sciences, University of North Carolina, Chapel Hill, NC 27599; and [b]College of Biological Sciences, China Agricultural University, Beijing 100193, China

Contributed by Jeffery L. Dangl, August 20, 2011 (sent for review August 9, 2011)

Plants and animals deploy intracellular immune receptors that perceive specific pathogen effector proteins and microbial products delivered into the host cell. We demonstrate that the ADR1 family of *Arabidopsis* nucleotide-binding leucine-rich repeat (NB-LRR) receptors regulates accumulation of the defense hormone salicylic acid during three different types of immune response: (*i*) ADRs are required as "helper NB-LRRs" to transduce signals downstream of specific NB-LRR receptor activation during effector-triggered immunity; (*ii*) ADRs are required for basal defense against virulent pathogens; and (*iii*) ADRs regulate microbial-associated molecular pattern-dependent salicylic acid accumulation induced by infection with a disarmed pathogen. Remarkably, these functions do not require an intact P-loop motif for at least one ADR1 family member. Our results suggest that some NB-LRR proteins can serve additional functions beyond canonical, P-loop–dependent activation by specific virulence effectors, extending analogies between intracellular innate immune receptor function from plants and animals.

nucleotide-binding domain and leucine-rich repeat-containing protein receptors | plant immune system | effector-triggered immunity | microbial-associated molecular pattern-triggered immunity

Plants respond to attempted microbial infection with a two-tiered immune system. In the first tier, extracellular pattern recognition receptors (PRRs) bind conserved microbial-associated molecular pattern (MAMP) ligands, activating a complex host response that results in MAMP-triggered immunity (MTI). Successful pathogens deploy suites of virulence effectors that delay or suppress MTI, allowing infection. In the second tier, plant intracellular immune receptors of the nucleotide-binding leucine-rich repeat (NB-LRR) protein family can be activated either by direct binding of effectors or, alternatively, by effector action on an associated target protein that generates a "modified-self" molecule (1, 2). Effector-mediated NB-LRR activation results in effector-triggered immunity (ETI), a rapid and high-amplitude output significantly overlapping with MTI (1). ETI is typically accompanied by the hypersensitive cell death response (HR), limited to the site of pathogen attack. Both MTI and some cases of NB-LRR–mediated ETI require the salicylic acid (SA)-signaling molecule as a downstream mediator of transcriptional output responses (3, 4).

Plant NB-LRR proteins belong to the STAND (signal transduction ATPases with numerous domains) superfamily, which includes the animal apoptotic proteins Apaf-1/CED4 and innate immune receptors of the nucleotide-binding domain and leucine-rich repeat-containing proteins (NLR) family (5). Animal NLRs are activated by MAMPs and by modified-self molecules in the form of danger-associated molecular patterns (6) and regulate inflammasome activation, autophagy, and cell death (7). STAND protein functions require an intact P-loop motif (GxxxxGKT/S) that coordinates ATP binding. STAND proteins are molecular switches that toggle from an ADP-bound "off" position to an ATP-bound "on" state that activates downstream signaling. Activation of both animal NLR and plant NB-LRR receptors results in intra- and intermolecular conformational changes driven by nucleotide binding and hydrolysis (8, 9).

Plant NB-LRR proteins studied to date function in ETI, although gain-of-function mutations or ectopic over-expression can lead to additional phenotypes (10). Epistatic interactions involving NB-LRR genes can result in autoimmune-like responses (11). In some cases, ETI responses require a pair of NB-LRR proteins, although it is unclear whether these proteins interact directly. In these cases, one NB-LRR acts as the genetically defined "effector-sensor" and the other is required for its function, but is not implicated in effector perception per se (12). We suggest the term "helper NB-LRRs" for the latter category. Recent phylogenetic evidence suggests that a small, but ancient, subclade of plant coiled-coil (CC_R)-NB-LRR proteins has evolved to fulfill "helper NB-LRR" function during ETI (13). Here, we demonstrate that the three members of the *Arabidopsis* CC_R-NB-LRR ADR1 protein family are helper NB-LRRs in ETI and function in basal defense and in response to a disarmed pathogen via regulation of SA accumulation and subsequent activation of SA-dependent responses. We further show, surprisingly, that the P-loop is dispensable for these functions, suggesting that CC_R-NB-LRR proteins can use an activation mechanism that differs from that of all other NB-LRR proteins studied to date in these contexts.

Results

***PHOENIX*21 Is a Positive Regulator of *lsd1* Runaway Cell Death and Is a Member of the ADR1 Family of CC_R-NB-LRR Proteins.** Mutants exist that cannot limit the spread of HR after NB-LRR activation. In the *Arabidopsis lsd1* (*l*esions *s*imulating *d*isease *1*) mutant, HR occurs normally, but the oxidative burst generated by pathogen recognition triggers a superoxide-dependent signal leading to "runaway cell death" that spreads beyond infection sites (14). This phenotype requires accumulation of SA and additional components of ETI/MTI signaling (15). In a screen for *lsd1* suppressors, we isolated mutations in the *PHOENIX* (*PHX*) loci. One recessive complementation group of two alleles (*phx21-1* and *phx21-2*) allowed neither the initiation nor the propagation of SA-induced *lsd1* runaway cell death in the Wassilewskija (Ws) ecotype (14) (Fig. S1 *A* and *B*). We isolated *PHX21* (At5g04720; hereafter, *ADR1-L2*) by map-based cloning (*SI Materials and Methods*). *ADR1-L2* encodes a CC_R-NB-LRR protein belonging to a small clade that includes ADR1 (*A*CTIVATED *D*ISEASE

Author contributions: V.B. and J.L.D. designed research; V.B., S.T., A.S., and M.R. performed research; V.B. and K.C. analyzed data; and V.B. and J.L.D. wrote the paper.

The authors declare no conflict of interest.

Freely available online through the PNAS open access option.

[1]To whom correspondence should be addressed. E-mail: dangl@email.unc.edu.

This article contains supporting information online at www.pnas.org/lookup/suppl/doi:10.1073/pnas.1113726108/-/DCSupplemental.

*R*ESISTANCE 1; At1g33560) and ADR1-L1 (At4g33300) (16) (Fig. S2*A*), previously characterized by the gain-of-function, over-expression phenotype of *adr1* (17, 18). Over-expression of ADR1 results in the constitutive activation of the defense responses as well as in drought tolerance; both of these phenotypes are SA-dependent (17, 18). Loss of function for *adr1-L1* results in modest suppression of ETI (19). We investigated ADR1 family functions in the Columbia (Col-0) ecotype after observing that an isogenic Col-0 allele (*adr1-L2-4*) also suppressed *lsd1* runaway cell death (Fig. S1 *C* and *D*).

ADR1 Proteins Function as Helper NB-LRRs for Some, but Not All, ETI Responses and Are Required for Basal Defense to Virulent Pathogens. We assessed whether the ADR1 proteins can function as helper NB-LRRs for well-defined NB-LRR–mediated ETI responses. We challenged *adr1*, *adr1-L1*, and *adr1-L2* single knock-out mutants (Fig. S2*B*), combinatorial double *adr1* mutants, and the *adr1 adr1-L1 adr1-L2* triple mutant (hereafter "*adr1* triple") with the bacterial pathogen *Pseudomonas syringae* pv. *tomato* (*Pto*) DC3000 expressing either the AvrRpm1 or AvrRpt2 effectors or with two isolates of the obligate biotrophic oomycete *Hyaloperonospora arabidopsidis* (*Hpa* isolates Emwa1 and Cala2). In Col-0, these effectors are recognized by either CC-NB-LRR proteins [RPM1 (20) and RPS2 (21)] or by the Toll/interleukin-1 receptor (TIR)-NB-LRR proteins [RPP4 (22) and RPP2 (23)], respectively. RPS2-mediated HR (Fig. 1*A* and Fig. S3*A*) and ETI (Fig. 1*B*) were significantly compromised in the *adr1* triple mutant. RIN4 cleavage by the cysteine protease effector AvrRpt2 (24), which initiates RPS2-mediated ETI, was maintained (Fig. S3*B*). Hence, the *ADR1* genes function downstream of this event in RPS2 signaling. Both RPP4- and RPP2-mediated ETI were also significantly compromised in the *adr1* triple mutant (Fig. 1 *C* and *D*) and weakly compromised in single and combinatorial mutants. The *adr1* triple mutant was nearly as susceptible to infection as the TIR-NB-LRR/basal defense signaling mutant *e*nhanced *d*isease *s*usceptibility 1 (*eds1*) (25). These results extend evidence that ADR1 and the NRG1 (*N r*equirement *g*ene *1*) CC_R-NB-LRR proteins are helper NB-LRRs (13). RPM1-mediated ETI was not altered (Fig. S4). Thus, some, but not all, effector-mediated ETI responses tested required ADR1 proteins.

NB-LRR protein function has been implicated in basal defense (26), which is activated by virulent pathogens on susceptible hosts and can limit pathogen growth (4). We thus tested the ability of the *adr1* family mutants to restrict the growth of virulent pathogens. The *adr1* triple mutant was more susceptible to *Hpa* Emco5 and to *Pto* DC3000 compared with wild-type or

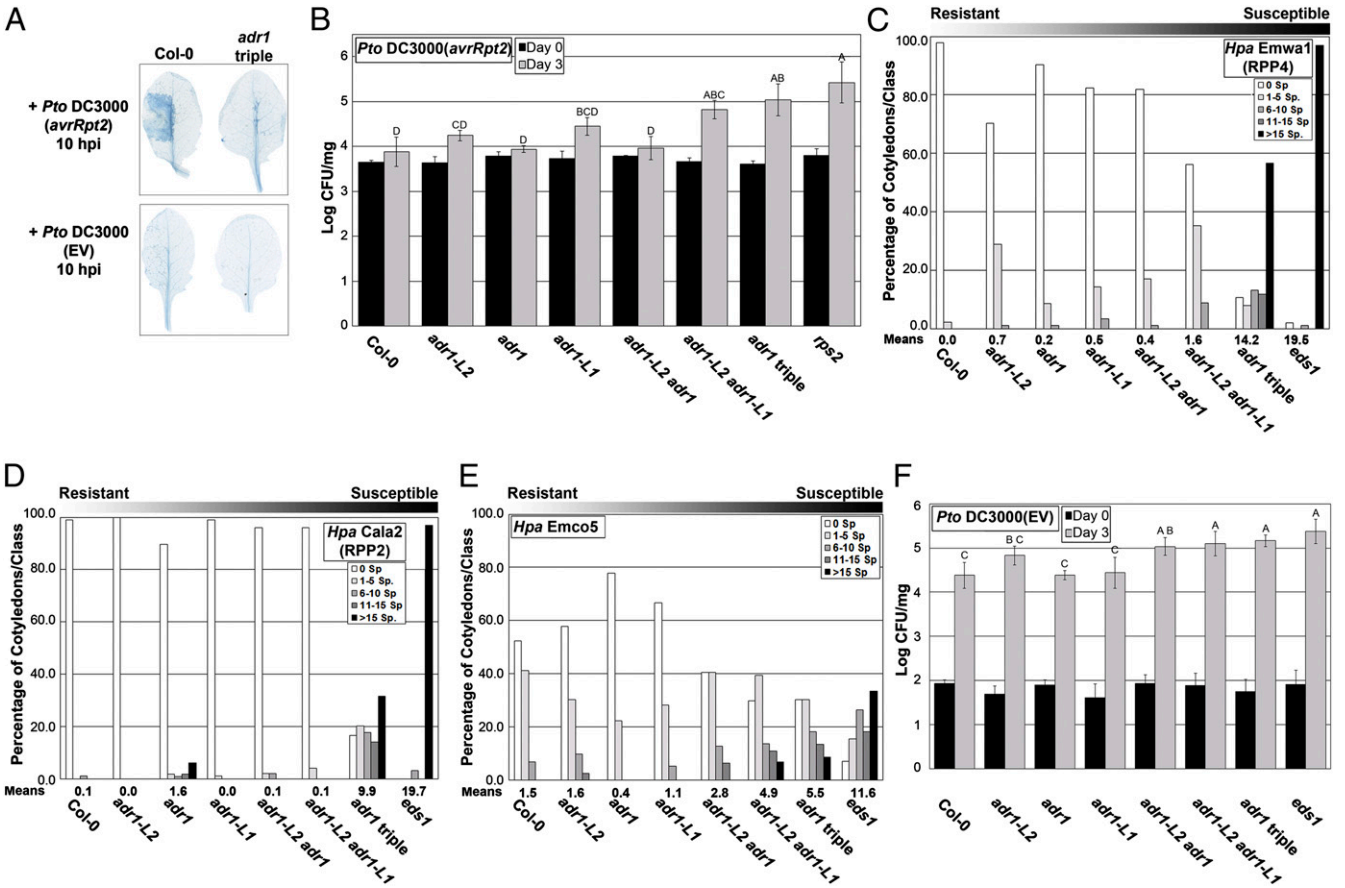

Fig. 1. ADR1 family members function in ETI and basal defense. (*A*) *Pto* DC3000(*avrRpt2*) or *Pto* DC3000(EV) (empty vector) was hand-infiltrated into leaves of 4-wk-old plants. Leaves were collected and stained with trypan blue to visualize cell death. (*B*) Twenty-day-old seedlings were dip-inoculated with *Pto* DC3000(*avrRpt2*), and bacterial growth was assessed at 0 and 3 d post inoculation (dpi). (*C*) Ten-day-old seedlings were inoculated with *Hpa* Emwa1. Sporangiophores per cotyledon were counted at 5 dpi (average of 100 cotyledons per genotype). Cotyledons were classified as supporting no sporulation (0 sporangiophores/cotyledon), light sporulation (1–5 and 6–10), medium sporulation (11–15), or heavy sporulation (>15). Means of sporangiophores/cotyledon for each genotype are noted below. (*D*) Ten-day-old seedlings were inoculated with *Hpa* Cala2. Sporangiophores/cotyledon were counted at 6 dpi as described above. (*E*) Ten-day-old seedlings were inoculated with *Hpa* Emco5. Sporangiophores/cotyledon were counted at 4 dpi as described above. (*F*) Twenty-day-old seedlings were dip-inoculated with *Pto* DC3000(EV). Bacterial growth was assessed at 0 and 3 dpi. Values in *B* and *F* are mean cfu/mg ± 2 × SE (n = 4). Letters indicate a significant difference following post-ANOVA Tukey's test (α = 0.05).

single *adr1* mutants (Fig. 1 *E* and *F*). Hence, ADR1 proteins act as redundant regulators of basal defense.

ADR1 Proteins Regulate SA Accumulation Following an Oxidative Burst. SA is a key downstream mediator of plant defense against biotrophic pathogens like those used here (27). Systemic acquired resistance (SAR) (28), basal defense (4), MTI (3), and some, but not all, NB-LRR–mediated ETI responses (29) require SA accumulation, which in turn controls transcriptional reprogramming through the BTB/POZ/ankyrin coactivator NPR1 (*N*onexpresser of *PR* genes *1*) (28). For example, RPS2 function is partially compromised in mutants that do not accumulate SA during ETI, but RPM1 is not.

An extracellular burst of superoxide derived from the NADPH oxidase AtrbohD and subsequent hydrogen peroxide (H_2O_2) production are also hallmarks of early MTI and ETI responses (30). In wild-type plants, this oxidative burst signals cells surrounding an infection site to up-regulate defense and anti-oxidant gene transcription and to down-regulate cell death (14, 31). Reactive oxygen and SA gradients surrounding an infection site are also part of a signal amplification system (32) that sets a cell death threshold controlled by LSD1 (30). We thus speculated that the ADR1 proteins might regulate SA homeostasis following an oxidative burst. Infection with *Pto* DC3000(*avrRpt2*) triggered an RPS2-dependent oxidative burst in the triple *adr1* triple mutant (Fig. 2 *A* and *B*). However, both free and total SA levels were poorly induced in this experiment, to levels as low as in either *rps2* or *eds1*, but slightly more than in the SA biosynthetic mutant *sid2* (Fig. 2*C*).

Provision of an SA analog (benzothiadiazole, or BTH) (33) rescued the defective ETI and basal defense responses of the *adr1* triple mutant. Pretreatment with BTH restored RPS2-dependent HR in the *adr1* triple mutant and the SA biosynthetic mutant *sid2* (Fig. 2*D*). BTH also rescued the enhanced susceptibility to *Pto* DC3000(EV) detected in both the *adr1* triple mutant and the *eds1* controls pretreated with water (Fig. 2*E*). This phenotype required NPR1. We conclude that these deficient ETI and basal defense responses are the consequences of the *adr1* triple mutant's inability to accumulate SA. Our results suggest that ADR1 proteins are required for SA accumulation following an intact oxidative burst upon effector and MAMP recognition.

HrpL-deficient *Pto* DC3000Δ*hrpL* is a potent MTI trigger because it cannot deliver MTI-suppressing effectors to the host (34). *Pto* DC3000Δ*hrpL* induced a weak, but detectable, oxidative burst (Fig. 2 *A* and *B*) sufficient to trigger SA accumulation in Col-0 (3), but not in the *adr1* triple mutant (Fig. 2*F*). Hence, recognition of one or more MAMPs expressed by *Pto* DC3000Δ*hrpL*

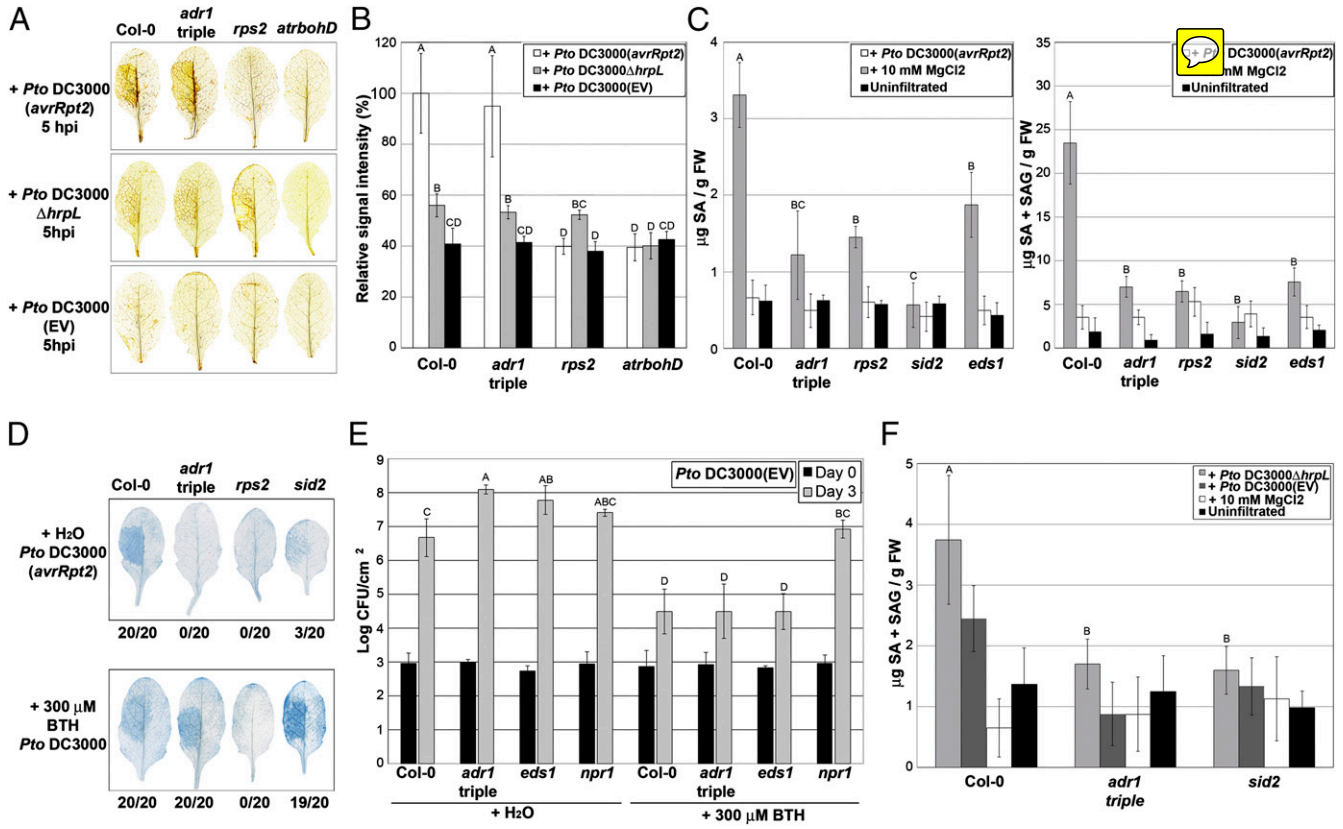

Fig. 2. ADR1 proteins are required for effector-independent SA accumulation following a superoxide burst. (*A*) Leaves from 4-wk-old plants were hand-infiltrated with *Pto* DC3000(*avrRpt2*), *Pto* DC3000Δ*hrpL*, or *Pto* DC3000(EV). H_2O_2 accumulation was monitored by 3′,3′-diaminobenzidine (DAB) staining at 5 h post inoculation (hpi). Leaves are representative of 10 individuals. (*B*) DAB staining shown in *A* was quantified (mean ± 2 × SE, $n = 5$). Letters indicate a significant difference following post-ANOVA Student's *t* test ($\alpha = 0.05$). (*C*) Leaves from 4-wk-old plants were hand-infiltrated with *Pto* DC3000(*avrRpt2*) or with $MgCl_2$. Free (*Left*) and total SA (*Right*) were measured at 24 hpi (mean ± 2 × SE, $n = 4$). (*D*) *Pto* DC3000(*avrRpt2*) was hand-infiltrated into leaves from 4-wk-old plants pretreated with either H_2O (*Upper*) or BTH (*Lower*) 24 h before bacterial infiltration. Leaves were collected 10 hpi and stained with trypan blue. Leaves are representative of 20 individuals. Numbers indicate how many leaves showed HR out of the total number of leaves analyzed. (*E*) Four-week-old plants were sprayed with either H_2O or BTH. Leaves were hand-infiltrated with *Pto* DC3000(EV) 2 d post application (dpa). Bacterial growth was monitored at 0 and 3 dpi, mean ± 2 × SE ($n = 4$). (*F*) Leaves from 4-wk-old plants were hand-infiltrated with *Pto* DC3000Δ*hrpL*, *Pto* DC3000(EV), or $MgCl_2$. Total SA was measured at 9 hpi (mean ± 2 × SE, $n = 4$) and compared with SA levels from uninfiltrated plants. Letters indicate a significant difference among genotypes infiltrated with *Pto* DC3000Δ*hrpL* following post-ANOVA Student's *t* test ($\alpha = 0.05$). The experiments in *A*–*F* were repeated three times with similar results.

activates MTI responses that result in SA accumulation regulated by the ADR1 proteins.

The two best-characterized MTI responses follow specific recognition of peptides derived from either bacterial flagellin (flg22) or elongation factor (elf18) by the PRRs FLS2 and EFR, respectively (35, 36). The accumulation of a functional epitope-tagged ADR1-L2 protein expressed from its native promoter was up-regulated by both flg22 and elf18 peptide treatments, as well as upon BTH application (Fig. S5), yet the *adr1* triple mutant exhibited normal oxidative burst, MAPK activation, and callose deposition following treatment with either peptide (Fig. S6). Collectively, these findings indicate that the ADR1 proteins act in MTI downstream or independently of early events subsequent to EFR or FLS2 activation but upstream of SA accumulation.

An Intact P-Loop Domain Is Dispensable for Any of the ADR1-L2 Functions. STAND proteins bind ATP and most act as ATPases. These include plant NB-LRR proteins (8), a variety of animal NLRs and cell death control proteins (5), and functionally diverse bacterial proteins (9). To date, there is no crystal structure of a full-length NB-LRR or NLR immune receptor. However, structures for both Apaf1 [a functional ATPase (37)] and CED4, which binds ATP (38) but does not hydrolyze it (39), are available (39, 40). Homology modeling of the CC_R-NB domain (residues 40–671) of ADR1-L2 with Apaf-1 (residues 1–586) confirmed the location of conserved functionally relevant glycine and lysine residues (GK212/213) analogous to Apaf-1 (GK159/160) in the ATP-binding pocket of the P-loop (Fig. S7 *A* and *B*). The P-loop directly interacts with the β-phosphate of ADP (41). An invariant GK residue pair is crucial for this interaction, and mutation of these residues abrogates nucleotide binding and/or ATPase activity and functions across kingdoms (41, 42) (Fig. S7*G*).

We constructed transgenic *adr1* triple-mutant transgenic plants expressing wild-type *ADR1-L2*, *ADR1-L2*$_{G212A}$, *ADR1-L2*$_{K213R}$, or *ADR1-L2*$_{AAA}$ (GKT212/213/214AAA) with C-terminal HA-epitope tags under the control of the native promoter (Fig. S7 *C–E*). Surprisingly, homozygous transgenic *adr1* triple-mutant lines expressing these alleles (Fig. 3*A*) complemented RPS2-mediated HR (Fig. 3*B*), RPP4-dependent ETI (Fig. 3*C*), basal defense (Fig. 3*D*), and *Pto* DC3000*ΔhrpL*-induced SA accumulation (Fig. 3*E*) to levels comparable to those observed in the *adr1 adr1-L1* double mutant. Thus, an intact P-loop motif is dispensable for

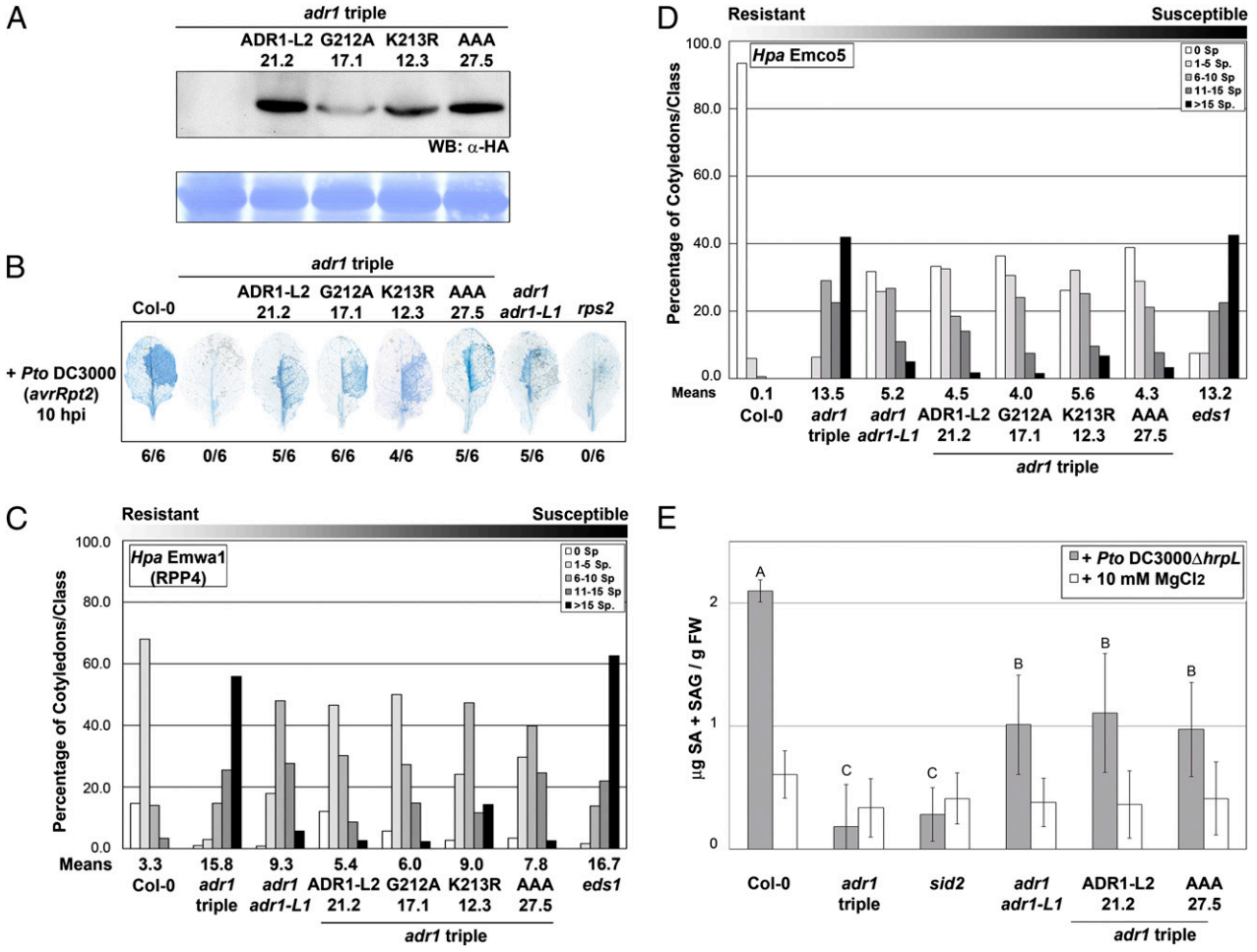

Fig. 3. An intact P-loop catalytic domain is dispensable for ADR1-L2 to function in ETI, basal defense, and MTI. (*A*) Protein extracts were sampled from stable homozygous transgenic *adr1* triple plants expressing HA-tagged *ADR1-L2*, *ADR1-L2*$_{G212A}$, *ADR1-L2*$_{K213R}$, or *ADR1-L2*$_{AAA}$ (*ADR1-L2*, *G212A*, *K213R*, *AAA*, respectively). Numbers indicate the identity of the transgenic lines used. An anti-HA antibody was used to detect ADR1-L2 protein accumulation. Equal loading was verified by Coomassie staining (*Lower*). (*B*) *Pto* DC3000(*avrRpt2*) was hand-infiltrated into leaves from 4-wk-old plants and stained with trypan blue. Numbers indicate how many leaves showed HR out of the total number of leaves analyzed. (*C*) Ten-day-old seedlings were inoculated with *Hpa* Emwa1. Sporangiophores/cotyledon were counted at 5 dpi, and cotyledons were classified as in Fig. 1. (*D*) Ten-day-old seedlings were inoculated with *Hpa* Emco5. Sporangiophores were counted at 4 dpi as above. (*E*) Leaves from 4-wk-old plants were hand-infiltrated with *Pto* DC3000*ΔhrpL* or $MgCl_2$. Total SA was measured at 9 hpi (mean ± 2 × SE, $n = 4$) and compared with SA levels from mock-treated plants. Letters indicate a significant difference among genotypes infiltrated with *Pto* DC3000*ΔhrpL* following post-ANOVA Student's *t* test (α = 0.05). The assays in *B–D* were repeated three times with similar results.

ADR1-L2 functions in ETI, basal defense, and MTI. Additionally, an allele of ADR1-L2 that lacks a functional P-loop can function in the absence of the other two ADR1 family members.

Discussion

We demonstrate that the CC_R-NB-LRR ADR1 proteins are functionally distinct innate plant immune receptors. They regulate SA-dependent defense in three contexts: MTI responses against a disarmed pathogen, basal defense against virulent pathogens, and some, but not all, ETI responses. Moreover, at least ADR1-L2 function in these contexts is P-loop–independent. Hence, ADR1-L2 is not activated via the canonical mechanism used by NB-LRR and NLR receptors as microbial sensors, at least for the phenotypes that we describe.

NB-LRR pairs acting in ETI have been reported (12). The lack of physical interaction between the pairs analyzed to date supports a scenario in which the helper NB-LRRs might constitute convergence points in defense responses downstream of recognition and oxidative burst mediated by either PRRs or by NB-LRR sensors activated via effector-driven, P-loop–dependent conformational changes. Our analysis of the CC_R-NB-LRR ADR1 proteins is consistent with their evolutionary history and divergence from other CC-NB-LRR family members (13).

We speculate that the CC_R-NB-LRR ADR1 proteins might function as signaling scaffolds and regulators of signal transduction processes leading to SA accumulation and consequent defense outputs. This is reminiscent of the function of NLRC5 and NLRP12, NLRs that do not function as microbial sensors per se but rather regulate intracellular signaling pathways (43). These proinflammatory NLRs might function in conjunction with additional NLRs, as suggested by the physical interaction of NLRP12 with NOD2 (44). By analogy, the plant CC_R-NB-LRR ADR1 proteins might mediate signal transduction in response to common upstream stimuli. Consequently, the microbial sensor function of immune receptors might be the result of the coordination between effector-mediated sensor activation and a more general signaling function provided by CC_R-NB-LRR ADR1 proteins.

The expanded CC_R-NB-LRR functions that we describe for at least ADR1-L2 require neither the canonical P-loop motif nor the other two full-length CC_R-NB-LRR ADR1 family members. We note the presence of *ADR1-L3* in the Col-0 genome (At5g47280), although it lacks approximately the first 190 amino acids at its N terminus and has no reported phenotype. Nevertheless, this protein could play a unique and equally noncanonical role in the phenotypes that we describe. We suggest that the unique signaling functions for at least ADR1-L2 are a consequence of its association with one or more yet-to-be-defined defense machines. The functions that we define for CC_R-NB-LRR ADR1 proteins do not preclude an additional, undiscovered, P-loop–dependent function as an effector sensor that, in this context, may associate with and guard the hypothetical signaling machine. Interestingly, a rice protein was recently described that lacks an intact ATP-binding domain and functions in disease resistance against rice blast (45), suggesting a mode of action similar to the CC_R-NB-LRR ADR1 proteins. We speculate that additional immune receptors of the NB-LRR and NLR classes might have the following mechanistically separable functions: (*i*) canonical P-loop–dependent activation via microbial perturbation of the inter- and intramolecular interactions that repress nucleotide exchange and/or hydrolysis and (*ii*) recognition-independent, P-loop–independent scaffold functioning as part of stress response machinery.

Materials and Methods

ADR1 CC_R-NB-LRR Protein Family Nomenclature. *ADR1* (At1g33560) was identified via its ectopic over-expression phenotype, which resulted in constitutive SA-dependent defense gene activation and consequent induction of disease resistance, a common NB-LRR protein gain-of-function phenotype. *ADR1-L1* (At4g33300) and *ADR1-L2* (At5g04720) were identified by homology (16).

Plant Lines and Pathogens Strains. T-DNA insertion lines in the *Arabidopsis thaliana* Col-0 accession were from public collections and were identified by searching the SiGNAL database (http://signal.salk.edu). Details of the mutants, the pathogen strains, and their growth quantification used in this study are provided in *SI Materials and Methods*.

DNA Manipulations. Standard techniques of DNA manipulation were used.

Cell Death Assays. Leaves were harvested and cell death was assessed by Trypan blue staining to visualize dead cells or by conductivity measurements as described in *SI Materials and Methods*.

Immunoblot Analysis. Leaves from 4-wk-old plants were harvested, and total proteins were extracted by grinding frozen tissue in a buffer containing 20 mM Tris·HCl (pH 7.0), 150 mM NaCl, 1 mM EDTA (pH 8.0), 1% Triton X-100, 0.1% SDS, 10 mM DTT, and plant protein protease inhibitor mixture (Sigma-Aldrich). Samples were centrifuged at 14,000 × *g* for 15 min at 4 °C to pellet the debris. Proteins (75 μg) were separated on 7.5% or 12% SDS/PAGE for detection of *ADR1-L2* or RIN4, respectively. Proteins were transferred to polyvinylidene difluoride membranes, and Western blots were performed using standard methods. Monoclonal anti-HA antibody (Santa Cruz Biotechnology) antibody was used at a 1:3,000 dilution, whereas anti-RIN4 serum was used at 1:2,000. Signals were detected by enhanced chemiluminescence using ECL Plus (Amersham Biosciences).

Detection of H_2O_2. H_2O_2 was visualized in situ by 3,3′-diaminobenzidine (DAB) staining as described (30). Leaves from 4-wk-old plants were hand-infiltrated with *Pto* DC3000(*avrRpt2*) or *Pto* DC3000Δ*hrpL* at 10^7 cfu/mL and collected 10 h after infiltration. Leaves were vacuum-infiltrated with a solution containing 1 mg/mL DAB and placed in a dark plastic box under high humidity for an additional 8 h. Leaves were then destained in a solution of 3:1:1 ethanol/lactic acid/glycerol.

Free and Total SA Measurement. Leaves from 4-wk-old plants were hand-infiltrated with *Pto* DC3000(*avrRpt2*) at 10^7 cfu/mL or with *Pto* DC3000Δ*hrpL* at 5×10^7 cfu/mL free SA and glucose-conjugated SA (SAG) (SA + SAG) measurements were performed as described in *SI Materials and Methods*.

ACKNOWLEDGMENTS. We thank Farid El Kasmi, Petra Epple, Marc Nishimura, and Nuria Sanchez-Coll for critical reading of the manuscript; Colleen Rice for technical support; Jane Parker for sharing *eds1-2* seeds; Xiaoyou Zheng for assistance with the SA measurement; Christopher Willet and Darrel Stafford for sharing equipment; Brian Nalley and Susan Whitfield for graphics assistance; and John Craig and Derek Werner for greenhouse assistance. J.L.D. is a Howard Hughes Medical Institute-Gordon and Betty Moore Foundation Plant Science Investigator. This work was funded by the National Institutes of Health (Grants RO1GM066025 and R01GM057171 with an American Recovery & Reinvestment Act supplement to J.L.D.) and the National Science Foundation (Arabidopsis 2010 Program Grant IOS-0929410 to J.L.D.); V.B. was supported by the Human Frontier Science Program (Grant LT00905/2006-L); S.T. was supported by the National Natural Science Foundation of China (Grant 30671180).

1. Jones JD, Dangl JL (2006) The plant immune system. *Nature* 444:323–329.
2. Dodds PN, Rathjen JP (2010) Plant immunity: Towards an integrated view of plant-pathogen interactions. *Nat Rev Genet* 11:539–548.
3. Tsuda K, Sato M, Glazebrook J, Cohen JD, Katagiri F (2008) Interplay between MAMP-triggered and SA-mediated defense responses. *Plant J* 53:763–775.
4. Glazebrook J (2005) Contrasting mechanisms of defense against biotrophic and necrotrophic pathogens. *Annu Rev Phytopathol* 43:205–227.
5. Leipe DD, Koonin EV, Aravind L (2004) STAND, a class of P-loop NTPases including animal and plant regulators of programmed cell death: Multiple, complex domain architectures, unusual phyletic patterns, and evolution by horizontal gene transfer. *J Mol Biol* 343:1–28.
6. Ting JP, Willingham SB, Bergstralh DT (2008) NLRs at the intersection of cell death and immunity. *Nat Rev Immunol* 8:372–379.
7. Philpott DJ, Girardin SE (2010) Nod-like receptors: Sentinels at host membranes. *Curr Opin Immunol* 22:428–434.
8. Takken FL, Tameling WI (2009) To nibble at plant resistance proteins. *Science* 324:744–746.
9. Danot O, Marquenet E, Vidal-Ingigliardi D, Richet E (2009) Wheel of life, wheel of death: A mechanistic insight into signaling by STAND proteins. *Structure* 17:172–182.

10. Tameling WI, Joosten MH (2007) The diverse roles of NB-LRR proteins in plants. *Physiol Mol Plant Pathol* 71:126–134.
11. Bomblies K, et al. (2007) Autoimmune response as a mechanism for a Dobzhansky-Muller-type incompatibility syndrome in plants. *PLoS Biol* 5:e236.
12. Eitas TK, Dangl JL (2010) NB-LRR proteins: Pairs, pieces, perception, partners, and pathways. *Curr Opin Plant Biol* 13:472–477.
13. Collier SM, Hamel LP, Moffett P (2011) Cell death mediated by the N-terminal domains of a unique and highly conserved class of NB-LRR protein. *Mol Plant Microbe Interact* 24:918–931.
14. Jabs T, Dietrich RA, Dangl JL (1996) Initiation of runaway cell death in an Arabidopsis mutant by extracellular superoxide. *Science* 273:1853–1856.
15. Aviv DH, et al. (2002) Runaway cell death, but not basal disease resistance, in lsd1 is SA- and NIM1/NPR1-dependent. *Plant J* 29:381–391.
16. Chini A, Loake GJ (2005) Motifs specific for the ADR1 NBS-LRR protein family in Arabidopsis are conserved among NBS-LRR sequences from both dicotyledonous and monocotyledonous plants. *Planta* 221:597–601.
17. Chini A, Grant JJ, Seki M, Shinozaki K, Loake GJ (2004) Drought tolerance established by enhanced expression of the CC-NBS-LRR gene, ADR1, requires salicylic acid, EDS1 and ABI1. *Plant J* 38:810–822.
18. Grant JJ, Chini A, Basu D, Loake GJ (2003) Targeted activation tagging of the Arabidopsis NBS-LRR gene, ADR1, conveys resistance to virulent pathogens. *Mol Plant Microbe Interact* 16:669–680.
19. Wang W, et al. (2011) Timing of plant immune responses by a central circadian regulator. *Nature* 470:110–114.
20. Mackey D, Holt BF, III (2002) Wiig A, Dangl JL (2002) RIN4 interacts with Pseudomonas syringae type III effector molecules and is required for RPM1-mediated resistance in Arabidopsis. *Cell* 108:743–754.
21. Mackey D, Belkhadir Y, Alonso JM, Ecker JR, Dangl JL (2003) Arabidopsis RIN4 is a target of the type III virulence effector AvrRpt2 and modulates RPS2-mediated resistance. *Cell* 112:379–389.
22. Holub EB, Beynon JL, Crute IR (1994) Phenotypic and genotypic characterization of interactions between isolates of Peronospora parasitica and accessions of Arabidopsis thaliana. *Mol Plant Microbe Interact* 7:223–239.
23. Holub EB, Beynon J (1997) Symbiology of mouse-ear cress (Arabidopsis thaliana) and oomycetes. *Adv Bot Res* 24:228–273.
24. Kim HS, et al. (2005) The Pseudomonas syringae effector AvrRpt2 cleaves its C-terminally acylated target, RIN4, from Arabidopsis membranes to block RPM1 activation. *Proc Natl Acad Sci USA* 102:6496–6501.
25. Feys BJ, Moisan LJ, Newman MA, Parker JE (2001) Direct interaction between the Arabidopsis disease resistance signaling proteins, EDS1 and PAD4. *EMBO J* 20: 5400–5411.
26. Holt BF, III (2005) Belkhadir Y, Dangl JL (2005) Antagonistic control of disease resistance protein stability in the plant immune system. *Science* 309:929–932.
27. Loake G, Grant M (2007) Salicylic acid in plant defence: The players and protagonists. *Curr Opin Plant Biol* 10:466–472.
28. Durrant WE, Dong X (2004) Systemic acquired resistance. *Annu Rev Phytopathol* 42: 185–209.
29. McDowell JM, et al. (2000) Downy mildew (Peronospora parasitica) resistance genes in Arabidopsis vary in functional requirements for NDR1, EDS1, NPR1 and salicylic acid accumulation. *Plant J* 22:523–529.
30. Torres MA, Jones JD, Dangl JL (2005) Pathogen-induced, NADPH oxidase-derived reactive oxygen intermediates suppress spread of cell death in Arabidopsis thaliana. *Nat Genet* 37:1130–1134.
31. Kliebenstein DJ, Dietrich RA, Martin AC, Last RL, Dangl JL (1999) LSD1 regulates salicylic acid induction of copper zinc superoxide dismutase in Arabidopsis thaliana. *Mol Plant Microbe Interact* 12:1022–1026.
32. Shirasu K, Nakajima H, Rajasekhar VK, Dixon RA, Lamb C (1997) Salicylic acid potentiates an agonist-dependent gain control that amplifies pathogen signals in the activation of defense mechanisms. *Plant Cell* 9:261–270.
33. Lawton KA, et al. (1996) Benzothiadiazole induces disease resistance in Arabidopsis by activation of the systemic acquired resistance signal transduction pathway. *Plant J* 10:71–82.
34. Block A, Alfano JR (2011) Plant targets for Pseudomonas syringae type III effectors: Virulence targets or guarded decoys? *Curr Opin Microbiol* 14:39–46.
35. Zipfel C, et al. (2006) Perception of the bacterial PAMP EF-Tu by the receptor EFR restricts Agrobacterium-mediated transformation. *Cell* 125:749–760.
36. Gómez-Gómez L, Boller T (2000) FLS2: An LRR receptor-like kinase involved in the perception of the bacterial elicitor flagellin in Arabidopsis. *Mol Cell* 5:1003–1011.
37. Hu Y, Benedict MA, Ding L, Núñez G (1999) Role of cytochrome c and dATP/ATP hydrolysis in Apaf-1-mediated caspase-9 activation and apoptosis. *EMBO J* 18: 3586–3595.
38. Chinnaiyan AM, Chaudhary D, O'Rourke K, Koonin EV, Dixit VM (1997) Role of CED-4 in the activation of CED-3. *Nature* 388:728–729.
39. Yan N, et al. (2005) Structure of the CED-4-CED-9 complex provides insights into programmed cell death in Caenorhabditis elegans. *Nature* 437:831–837.
40. Riedl SJ, Li W, Chao Y, Schwarzenbacher R, Shi Y (2005) Structure of the apoptotic protease-activating factor 1 bound to ADP. *Nature* 434:926–933.
41. Hanson PI, Whiteheart SW (2005) AAA+ proteins: Have engine, will work. *Nat Rev Mol Cell Biol* 6:519–529.
42. Tameling WI, et al. (2002) The tomato R gene products I-2 and MI-1 are functional ATP binding proteins with ATPase activity. *Plant Cell* 14:2929–2939.
43. Kufer TA, Sansonetti PJ (2011) NLR functions beyond pathogen recognition. *Nat Immunol* 12:121–128.
44. Wagner RN, Proell M, Kufer TA, Schwarzenbacher R (2009) Evaluation of Nod-like receptor (NLR) effector domain interactions. *PLoS ONE* 4:e4931.
45. Hayashi N, et al. (2010) Durable panicle blast-resistance gene Pb1 encodes an atypical CC-NBS-LRR protein and was generated by acquiring a promoter through local genome duplication. *Plant J* 64:498–510.

Supporting Information

Bonardi et al. 10.1073/pnas.1113726108

SI Materials and Methods

Plant Lines and Propagation. All *Arabidopsis* mutant lines are in the Columbia (Col-0) ecotype except *lsd1-1* (1), which is in the Wassilewskija (Ws) accession. *adr1-L2-4* (At5g04720, SALK_126422), *adr1-L2-6* (SALK_150245), *adr1-1* (At1g33560, SAIL_842_B05), and *adr1-L1-1* (At4g33300, SAIL_302_C06) were obtained from the *Arabidopsis* Biological Resource Center. *atrbohD* (2), *lsd1-2* (3), *npr1-1* (4), *rps2-101C* (5), *rpm1-3* (6), *sid2-1* (7), *fls2* (8), and *efr* (8) are described elsewhere. The Col-0 *eds1-2* introgressed line was provided by Jane Parker (Max-Planck-Institut for Plant Breeding Research, Cologne, Germany). Plants were grown under short-day conditions (9 h light, 21 °C; 15 h dark, 18 °C).

Mapping. *phx21-2* was mapped by map-based cloning. A mapping population was generated from the F2 plants derived from a cross between the Col-0 introgressed $lsd1^C$ (9) and *phx21-2 lsd1-1*. A total of 100 F2 plants were obtained by prescreening with benzothiadiazole (BTH) spraying. Genetic analysis showed that *phx21-2* was recessive (130 wild type, 54 mutant, $\chi^2 = 1.86$, $P > 0.2$). The F2 suppressor was allowed to self and was confirmed in the F3 generation. DNA from 10 F2 individuals was used in PCR amplification of known PCR-based molecular markers (http://www.arabidopsis.org) to obtain approximate mapping positions. This interval was refined using molecular markers that we developed (available upon request). We used DNA from F2 individuals to find a clear linkage of *phx21-2* to the top arm of chromosome 5 between the molecular markers F15F17-5 and ciw18. Proof of isolation was obtained via sequence analysis of independent mutant alleles, as noted in the main text.

DNA Manipulations and Generation of Transgenic Plants. For expression of *ADR1-L2*, $ADR1\text{-}L2_{G212A}$, $ADR1\text{-}L2_{K213R}$, or $ADR1\text{-}L2_{AAA}$ under the control of its native promoter, *ADR1-L2-HA*, $ADR1\text{-}L2_{G212A}$-*HA*, $ADR1\text{-}L2_{K213R}$-*HA*, or $ADR1\text{-}L2_{AAA}$-*HA* cDNAs were fused by PCR to *ADR1-L2* promoter (500 bp) and cloned in the pGWB1 Gateway vector (10) for expression in the triple *adr1* mutant. *Arabidopsis* transgenics were generated using *Agrobacterium* (GV3101)-mediated transformation by floral dip (11).

Pathogen Strains, Inoculation, and Growth Quantification. *Hyaloperonospora arabidopsidis* (*Hpa*) isolates Emwa1 and Emco5 were propagated on the susceptible *Arabidopsis* ecotype Ws, whereas Cala2 was propagated on Ler. Conidiospores of *Hpa* Emwa1, Cala2, and Emco5 were resuspended in water at a concentration of 5×10^4 spores/mL and spray-inoculated onto 14-d-old seedlings (12). Inoculated plants were covered with a lid to increase humidity and grown at 19 °C under a 9-h light period.

Pto DC3000(EV) was resuspended in 10 mM $MgCl_2$ to a final concentration of 2.5×10^5 cfu/mL, whereas *Pto* DC3000 (*avrRpt2*) and *Pto* DC3000(*avrRpm1*) were resuspended to 2.5×10^7 cfu/mL. Twenty-day-old seedlings were dipped in the bacterial solution and growth was assessed as described (13). To test BTH-mediated acquired resistance, 4-wk-old plants were sprayed with a solution of 300 μM BTH or H_2O containing 0.005% Silwet. Leaves were hand-infiltrated with *Pto* DC3000 (EV) to 5×10^4 2 d post application (dpa), and bacterial growth was measured as described (14). To test the hypersensitive cell death response (HR), bacteria were resuspended in 10 mM $MgCl_2$ to 5×10^7 cfu/mL and hand-infiltrated in leaves from 4-wk-old plants. The RPM1- and RPS2-mediated HR was assessed at 5 and 10 h post inoculation (hpi), respectively.

Cell Death Assays. Leaves were harvested and stained with lactophenol trypan blue to visualize dead cells as described (12, 15). For the conductivity measurements (3, 16), leaves of 4-wk-old plants were infiltrated with the bacterial pathogens (see below) and at 1 hpi four leaf discs were cored (7-mm diameter), floated in water for 30 min, and subsequently transferred to tubes containing 6 mL distilled water. Conductivity of the solution was determined with an Orion conductivity meter at the indicated time points.

Free and Total Salicylic Acid Measurements. Free salicylic acid (SA) and glucose-conjugated SA (SAG) measurements were performed as described (17). Leaves (100 mg) were collected at 24 hpi [*Pto* DC3000(*avrRpt2*)] or 9 hpi (*Pto* DC3000Δ*hrpL*) and frozen in liquid nitrogen. Samples were ground and tissue was homogenized in 200 μL 0.1 M acetate buffer (pH 5.6). Samples were then centrifuged for 15 min at 16,000 × *g* at 4 °C. Supernatant (100 μL) was transferred to a new tube for free SA measurements, and 10 μL was incubated with 1 μL 0.5 U/μL β-glucosidase for 90 min at 37 °C for total SA measurement. After incubation, plant extracts were diluted fivefold with 44 μL acetate buffer for free SA measurement. Sixty microliters of LB media, 5 μL of plant extract (treated or not with β-glucosidase), and 50 μL of *Acinetobacter* sp. ADPWH-*lux* (OD = 0.4) were added to each well of a black 96-well plate. The plate was incubated at 37 °C for 60 min, and luminescence was read with the Spectra Max M5 (Molecular Devices) microplate reader.

For the standard curve, 1 μL of the known amount of SA stock (0–1,000 μg/mL) was diluted 10-fold in *sid2-1* plant extract, and 5 μL of each standard (undiluted for free SA measurement, or fivefold diluted for total SA) was added to the wells of the plate containing 60 μL of LB and 50 μL of *Acinetobacter* sp. ADPWH-*lux* (OD = 0.4). SA standards were read in parallel with the experimental samples.

Bioassays for Microbial-Associated Molecular Pattern-Induced Responses. The oxidative burst upon microbial-associated molecular pattern (MAMP) application was performed essentially as described previously (8). Leaf discs (3.8-mm diameter) excised from leaves of 4-wk-old plants were floated in water overnight. Water was replaced by a solution containing 100 nM flg22 or elf18, 17 μg/mL luminol (Sigma) and 10 μg/mL HRP (Sigma). Luminescence was recorded over time using the Spectra Max M5 (Molecular Devices) microplate reader. The MAPK activation assay was performed as described (18) with some modifications. Seven-day-old seedlings were grown in Murashige and Skoog (MS) agar plates and transferred for one additional week to MS liquid culture. The media were replaced with fresh liquid MS containing 1 μM of either flg22 or elf18. Seedlings were collected at the indicated time points, and proteins were extracted in a buffer containing 50 mM Tris·HCl (pH 7.5), 10 mM MgCl2, 15 mM EGTA, 100 mM NaCl, 2 mM DTT, 1 mM NaF, 1 mM Na_2MoO_4, 0.5 mM Na_3VO_4, 30 mM β-glycero-phosphate, and 0.1% Nonidet P-40. Samples were centrifuged at 16,000 × *g* for 30 min at 4 °C, and the supernatant was filtered through a layer of miracloth. Protein (40 μg) was loaded on a 12% SDS/PAGE. Membranes were probed with anti-phospho-p44/42 MAPK antibody (Cell Signaling).

MAMP-triggered callose deposition was also performed as described (19). flg22 and elf18 were applied at 2 or 1 μM, respectively, for 20 h on 2-wk-old seedlings, grown under the same conditions as for the MAPK activation assay. Seedlings were vacuum-infiltrated with 3:1 ethanol:glacial acetic acid and left shaking with several changes of solution for 8 h until cotyledons were translucent. Seedlings were then rehydrated in 70% ethanol for 2 h and in 50% ethanol for an additional 2 h, washed in water twice, and left shaking in water overnight. The following day, seedlings were washed twice in H_2O and incubated in 150 mM K_2HPO_4 (pH 9.5) containing 0.01% aniline blue for 4 h. Stained cotyledons were mounted on slides with 50% glycerol and viewed on a Nikon Eclipse E800 microscope under UV illumination with a broadband DAPI filter set. Flg22 and elf18 peptides were synthesized at the University of North Carolina (Chapel Hill, NC) Microprotein Sequencing and Peptide Synthesis core facility using the following sequences: QRLSTGSRINSAKDDAAGLQIA (flg22) and acetyl-SKEKFERTKPHVNVGTIG (elf18).

Molecular Modeling. A homology model for ADR1-L2 (residues 40–671) was constructed using an alignment to the crystal structure of ADP-bound Apaf-1 (residues 1–586) (Protein Data Bank ID 1Z6T) generated by the BioInfoBank Meta Server, a prediction-based server for protein structure and function (http://meta.bioinfo.pl) (20) and the MODELER 9v8 comparative modeling program (http://www.salilab.org/modeller/about_modeller.html) (21).

1. Dietrich RA, Richberg MH, Schmidt R, Dean C, Dangl JL (1997) A novel zinc finger protein is encoded by the Arabidopsis LSD1 gene and functions as a negative regulator of plant cell death. *Cell* 88:685–694.
2. Torres MA (2010) ROS in biotic interactions. *Physiol Plant* 138:414–429.
3. Torres MA, Jones JD, Dangl JL (2005) Pathogen-induced, NADPH oxidase-derived reactive oxygen intermediates suppress spread of cell death in Arabidopsis thaliana. *Nat Genet* 37:1130–1134.
4. Cao H, Glazebrook J, Clarke JD, Volko S, Dong X (1997) The Arabidopsis NPR1 gene that controls systemic acquired resistance encodes a novel protein containing ankyrin repeats. *Cell* 88:57–63.
5. Bent AF, et al. (1994) RPS2 of Arabidopsis thaliana: A leucine-rich repeat class of plant disease resistance genes. *Science* 265:1856–1860.
6. Grant MR, et al. (1995) Structure of the Arabidopsis RPM1 gene enabling dual specificity disease resistance. *Science* 269:843–846.
7. Wildermuth MC, Dewdney J, Wu G, Ausubel FM (2001) Isochorismate synthase is required to synthesize salicylic acid for plant defence. *Nature* 414:562–565.
8. Zipfel C, et al. (2006) Perception of the bacterial PAMP EF-Tu by the receptor EFR restricts Agrobacterium-mediated transformation. *Cell* 125:749–760.
9. Rustérucci C, Aviv DH, Holt BF, III, Dangl JL, Parker JE (2001) The disease resistance signaling components EDS1 and PAD4 are essential regulators of the cell death pathway controlled by LSD1 in Arabidopsis. *Plant Cell* 13:2211–2224.
10. Nakagawa T, et al. (2007) Development of series of gateway binary vectors, pGWBs, for realizing efficient construction of fusion genes for plant transformation. *J Biosci Bioeng* 104:34–41.
11. Clough SJ, Bent AF (1998) Floral dip: A simplified method for Agrobacterium-mediated transformation of Arabidopsis thaliana. *Plant J* 16:735–743.
12. Koch E, Slusarenko A (1990) Arabidopsis is susceptible to infection by a downy mildew fungus. *Plant Cell* 2:437–445.
13. Tornero P, Dangl JL (2001) A high-throughput method for quantifying growth of phytopathogenic bacteria in Arabidopsis thaliana. *Plant J* 28:475–481.
14. Morel JB, Dangl JL (1999) Suppressors of the Arabidopsis lsd5 cell death mutation identify genes involved in regulating disease resistance responses. *Genetics* 151:305–319.
15. Keogh RC, Deverall BJ, McLeod S (1980) Comparison of histological and physiological responses to Phakopsora pachyrhizi in resistant and susceptibal soybean. *Trans Br Mycol Soc* 74:329–333.
16. Dellagi A, Brisset MN, Paulin JP, Expert D (1998) Dual role of desferrioxamine in Erwinia amylovora pathogenicity. *Mol Plant Microbe Interact* 11:734–742.
17. Defraia CT, Schmelz EA, Mou Z (2008) A rapid biosensor-based method for quantification of free and glucose-conjugated salicylic acid. *Plant Methods* 4:28.
18. Lu X, et al. (2009) Uncoupling of sustained MAMP receptor signaling from early outputs in an Arabidopsis endoplasmic reticulum glucosidase II allele. *Proc Natl Acad Sci USA* 106:22522–22527.
19. Clay NK, Adio AM, Denoux C, Jander G, Ausubel FM (2009) Glucosinolate metabolites required for an Arabidopsis innate immune response. *Science* 323:95–101.
20. Ginalski K, Elofsson A, Fischer D, Rychlewski L (2003) 3D-Jury: A simple approach to improve protein structure predictions. *Bioinformatics* 19:1015–1018.
21. Eswar N, et al. (2006) Comparative protein structure modeling using Modeller. *Curr Protoc Bioinformatics* Chapter 5:Unit 5.6.
22. Chini A, Loake GJ (2005) Motifs specific for the ADR1 NBS-LRR protein family in Arabidopsis are conserved among NBS-LRR sequences from both dicotyledonous and monocotyledonous plants. *Planta* 221:597–601.
23. Jabs T, Dietrich RA, Dangl JL (1996) Initiation of runaway cell death in an Arabidopsis mutant by extracellular superoxide. *Science* 273:1853–1856.
24. Chisholm ST, et al. (2005) Molecular characterization of proteolytic cleavage sites of the Pseudomonas syringae effector AvrRpt2. *Proc Natl Acad Sci USA* 102:2087–2092.
25. Kim HS, et al. (2005) The Pseudomonas syringae effector AvrRpt2 cleaves its C-terminally acylated target, RIN4, from Arabidopsis membranes to block RPM1 activation. *Proc Natl Acad Sci USA* 102:6496–6501.
26. Riedl SJ, Li W, Chao Y, Schwarzenbacher R, Shi Y (2005) Structure of the apoptotic protease-activating factor 1 bound to ADP. *Nature* 434:926–933.
27. Tornero P, Chao RA, Luthin WN, Goff SA, Dangl JL (2002) Large-scale structure-function analysis of the Arabidopsis RPM1 disease resistance protein. *Plant Cell* 14: 435–450.
28. Scholz B, Rechter S, Drach JC, Townsend LB, Bogner E (2003) Identification of the ATP-binding site in the terminase subunit pUL56 of human cytomegalovirus. *Nucleic Acids Res* 31:1426–1433.
29. Gruver AM, et al. (2005) The ATPase motif in RAD51D is required for resistance to DNA interstrand crosslinking agents and interaction with RAD51C. *Mutagenesis* 20: 433–440.
30. Duncan JA, et al. (2007) Cryopyrin/NALP3 binds ATP/dATP, is an ATPase, and requires ATP binding to mediate inflammatory signaling. *Proc Natl Acad Sci USA* 104: 8041–8046.
31. Ye Z, et al. (2008) ATP binding by monarch-1/NLRP12 is critical for its inhibitory function. *Mol Cell Biol* 28:1841–1850.
32. Bendahmane A, Farnham G, Moffett P, Baulcombe DC (2002) Constitutive gain-of-function mutants in a nucleotide binding site-leucine rich repeat protein encoded at the Rx locus of potato. *Plant J* 32:195–204.
33. Inohara N, et al. (1999) Nod1, an Apaf-1-like activator of caspase-9 and nuclear factor-kappaB. *J Biol Chem* 274:14560–14567.
34. Faustin B, et al. (2007) Reconstituted NALP1 inflammasome reveals two-step mechanism of caspase-1 activation. *Mol Cell* 25:713–724.
35. Tameling WI, et al. (2002) The tomato R gene products I-2 and MI-1 are functional ATP binding proteins with ATPase activity. *Plant Cell* 14:2929–2939.
36. Gabriëls SH, et al. (2007) An NB-LRR protein required for HR signalling mediated by both extra- and intracellular resistance proteins. *Plant J* 50:14–28.
37. Dinesh-Kumar SP, Tham WH, Baker BJ (2000) Structure-function analysis of the tobacco mosaic virus resistance gene N. *Proc Natl Acad Sci USA* 97:14789–14794.
38. Tao Y, Yuan F, Leister RT, Ausubel FM, Katagiri F (2000) Mutational analysis of the Arabidopsis nucleotide binding site-leucine-rich repeat resistance gene RPS2. *Plant Cell* 12:2541–2554.
39. Ade J, DeYoung BJ, Golstein C, Innes RW (2007) Indirect activation of a plant nucleotide binding site-leucine-rich repeat protein by a bacterial protease. *Proc Natl Acad Sci USA* 104:2531–2536.
40. Howles P, et al. (2005) Autoactive alleles of the flax L6 rust resistance gene induce non-race-specific rust resistance associated with the hypersensitive response. *Mol Plant Microbe Interact* 18:570–582.
41. Chaudhary D, O'Rourke K, Chinnaiyan AM, Dixit VM (1998) The death inhibitory molecules CED-9 and CED-4L use a common mechanism to inhibit the CED-3 death protease. *J Biol Chem* 273:17708–17712.
42. Chinnaiyan AM, Chaudhary D, O'Rourke K, Koonin EV, Dixit VM (1997) Role of CED-4 in the activation of CED-3. *Nature* 388:728–729.
43. Kanuka H, et al. (1999) Proapoptotic activity of Caenorhabditis elegans CED-4 protein in Drosophila: Implicated mechanisms for caspase activation. *Proc Natl Acad Sci USA* 96:145–150.
44. Deyrup AT, Krishnan S, Cockburn BN, Schwartz NB (1998) Deletion and site-directed mutagenesis of the ATP-binding motif (P-loop) in the bifunctional murine ATP-sulfurylase/adenosine 5′-phosphosulfate kinase enzyme. *J Biol Chem* 273:9450–9456.
45. Babst M, Wendland B, Estepa EJ, Emr SD (1998) The Vps4p AAA ATPase regulates membrane association of a Vps protein complex required for normal endosome function. *EMBO J* 17:2982–2993.
46. Stephens KM, Roush C, Nester E (1995) Agrobacterium tumefaciens VirB11 protein requires a consensus nucleotide-binding site for function in virulence. *J Bacteriol* 177: 27–36.
47. Delepelaire P (1994) PrtD, the integral membrane ATP-binding cassette component of the Erwinia chrysanthemi metalloprotease secretion system, exhibits a secretion signal-regulated ATPase activity. *J Biol Chem* 269:27952–27957.

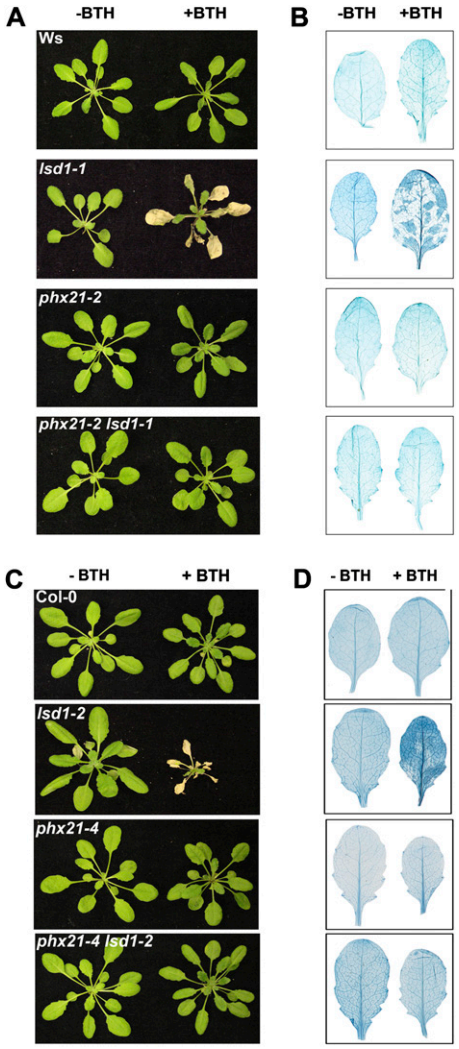

Fig. S1. ADR1-L2 positively regulates *lsd1* runaway cell death in Ws and Col-0. (*A* and *C*) Four-week-old plants were sprayed with 300 μM BTH, and pictures of the plants were taken 5 dpa. Untreated control plants of the same genotype are shown on the left. (*B* and *D*) Representative leaves of the plants shown in *A* and *C*, respectively, were stained with trypan blue to visualize the cell death at 5 dpa. All of the genotypes in *A* and *B* are in the Ws ecotype, whereas the genotypes in *C* and *D* are in the Col-0 accession.

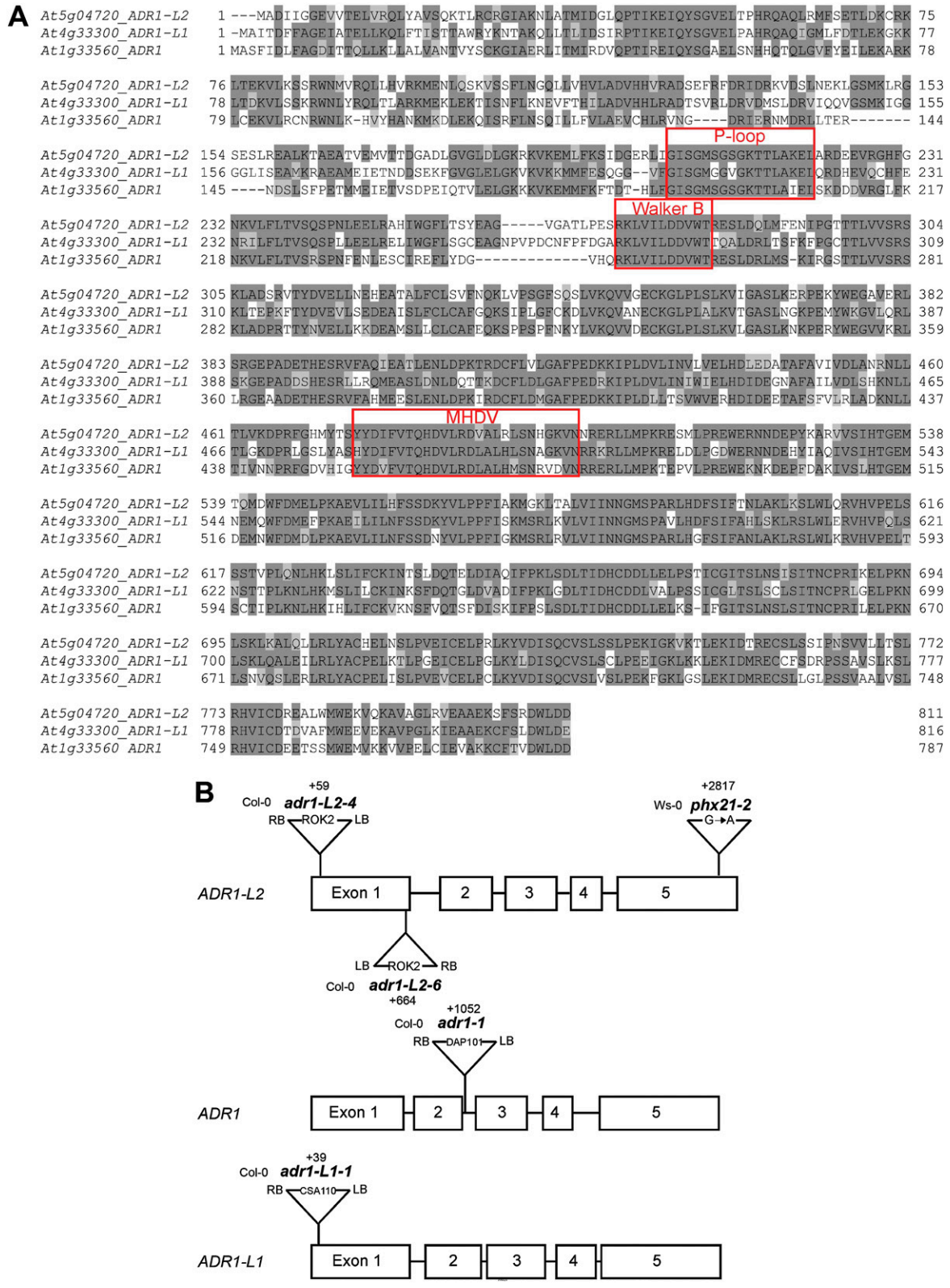

Fig. S2. ADR1-L2 is part of a small clade of coiled-coil nucleotide-binding leucine-rich repeat (CC_R-NB-LRR) proteins. (*A*) Alignment of the Col-0 ADR1 family deduced protein sequences. Sequences were aligned using ClustalW (http://www.ebi.ac.uk/Tools/clustalw/), and the alignment was edited with Jalview (http://www.jalview.org/index.html). Amino acids shaded in dark gray are invariant, whereas residues shaded in light gray are conserved in >60% of the sequences. The red boxes represent previously reported conserved motifs on the NB domains (22). (*B*) Mutations of *ADR1-L2*, *ADR1*, and *ADR1-L1* genes. The translated parts of exons (boxes), as well as intron sequences (lines), are depicted. For each T-DNA mutant used in this study, the insertion site and the orientation of the T-DNA are indicated. The corresponding lines were identified in the SALK or SAIL T-DNA collections and are in the Col-0 background: *adr1-L2-4*, SALK_126422; *ADR1-L2-6*, SALK_150245; *adr1-1*, SAIL_842_B05; and *adr1-L1-1*, SAIL_302_C06. The T-DNA insertions are not drawn to scale. *phx21-2* is the original EMS allele isolated in the Ws background (23), which carries a point mutation at the position 2,817 (G > A) that results in a premature stop codon. The numbers on top represent the position of the insertion or the mutation.

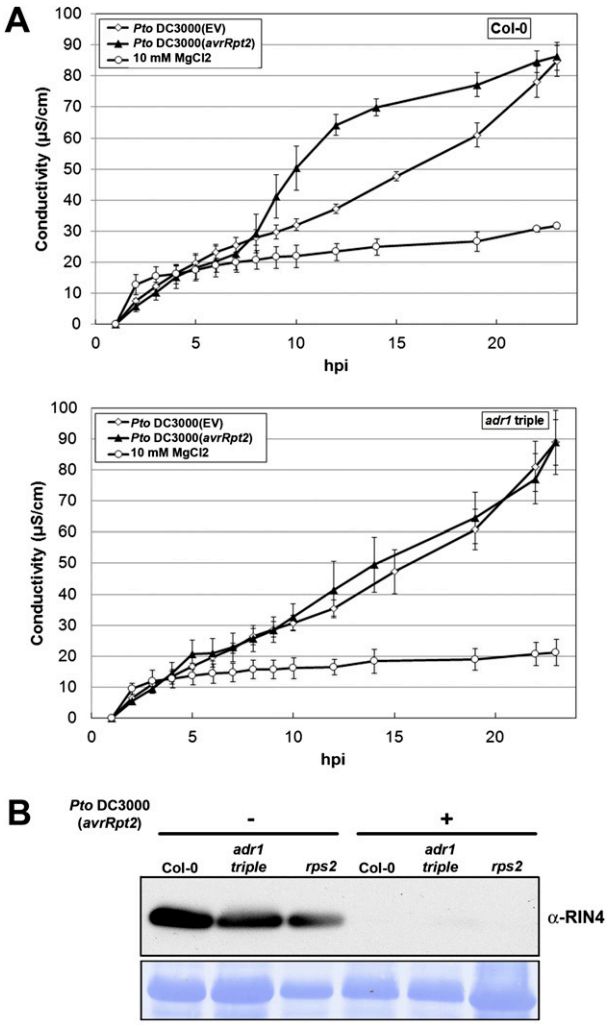

Fig. S3. ADR1 proteins function downstream of RIN4 cleavage in RPS2-mediated effector-triggered immunity (ETI). (*A*) Ion leakage measurements following inoculation with *Pto* DC3000 carrying EV, *avrRpt2*, or buffer only in Col-0 (*Upper*) or the triple *adr1* mutant (*Lower*). Following infiltration, four leaf discs per treatment were washed with H_2O for 30 min and then transferred to fresh H_2O where conductance was measured (µSiemens/cm) over time. Values are means ± 2 × SE (n = 5). The experiment is representative of three replicates. (*B*) Col-0 or triple *adr1* plants were hand-infiltrated with *Pto* DC3000(*avrRpt2*) (+) or 10 mM $MgCl_2$ (–).The cysteine protease type II effector AvrRpt2 targets and cleaves RIN4, leading to RPS2-mediated ETI (24, 25). Samples were collected at 24 hpi, and total protein extracts were subjected to anti-RIN4 Western blot to detect RIN4 cleavage.

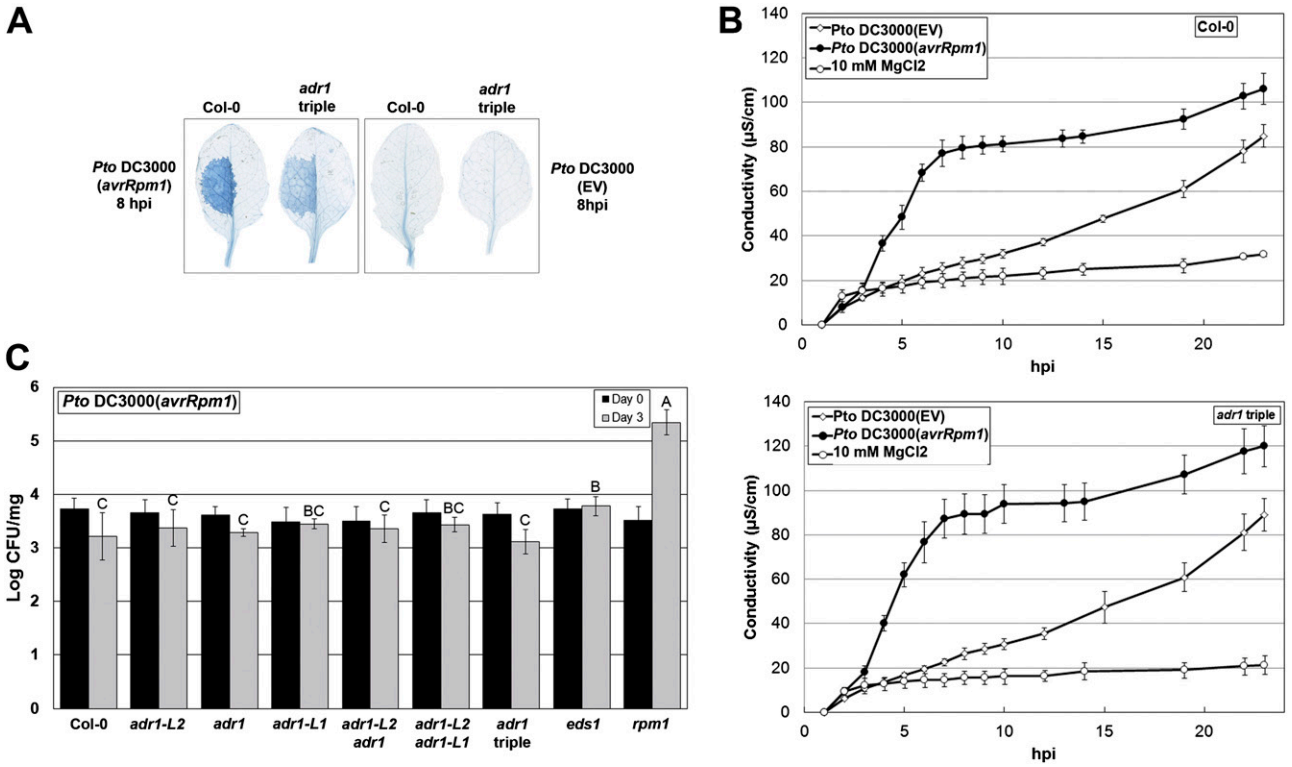

Fig. S4. ADR1 proteins are not required for RPM1-mediated effector-triggered immunity. (*A*) *Pto* DC3000(EV), or expressing *avrRpm1*, was hand-infiltrated into leaves from 4-wk-old plants. Leaves were collected at the indicated time and HR cell death was stained with TB. Leaves infiltrated with *Pto* DC3000(EV) do not show any cell death; thus the stain is specific for HR. (*B*) Ion leakage measurements following inoculation with *Pto* DC3000 carrying EV, *avrRpm1*, or buffer only in Col-0 (*Upper*) or the triple *adr1* mutant (*Lower*) were performed as in Fig. S3. Values are means ± 2 SE ($n = 5$). The experiment is representative of three replicates. (*C*) Fourteen-day-old seedlings of the genotypes listed were dip-inoculated with *Pto* DC3000 expressing *avrRpm1*, and bacterial growth was assessed at 0 and 3 dpi. Values are mean cfu/mg ± 2 × SE ($n = 4$). Letters indicate a significant difference following post-ANOVA Tukey's test ($\alpha = 0.05$).

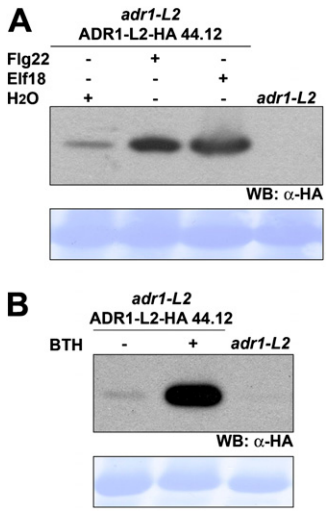

Fig. S5. ADR1-L2 expression is up-regulated by flg22, elf18, and BTH. (*A*) Seven-day old seedlings were grown on MS plates and transferred to liquid media for an additional week. A total of 1 μM flg22 or elf18 was added to fresh media, and proteins were sampled at 24 hpa. *adr1-L2* ADR1-L2-HA 44.12 represents a homozygous transgenic line of *adr1-L2* expressing a native copy of a C-terminally HA-tagged *ADR1-L2* allele. Anti-HA antibody was used to detect ADR1-L2 protein accumulation. Equal loading was verified by Coomassiee staining (*Lower*). (*B*) Four-week-old plants were sprayed with 300 μM BTH or mock-sprayed, and proteins were sampled at 24 hpa. Anti-HA was used to detect ADR1-L2 protein accumulation. Equal loading was ensured by Coomassiee staining (*Lower*).

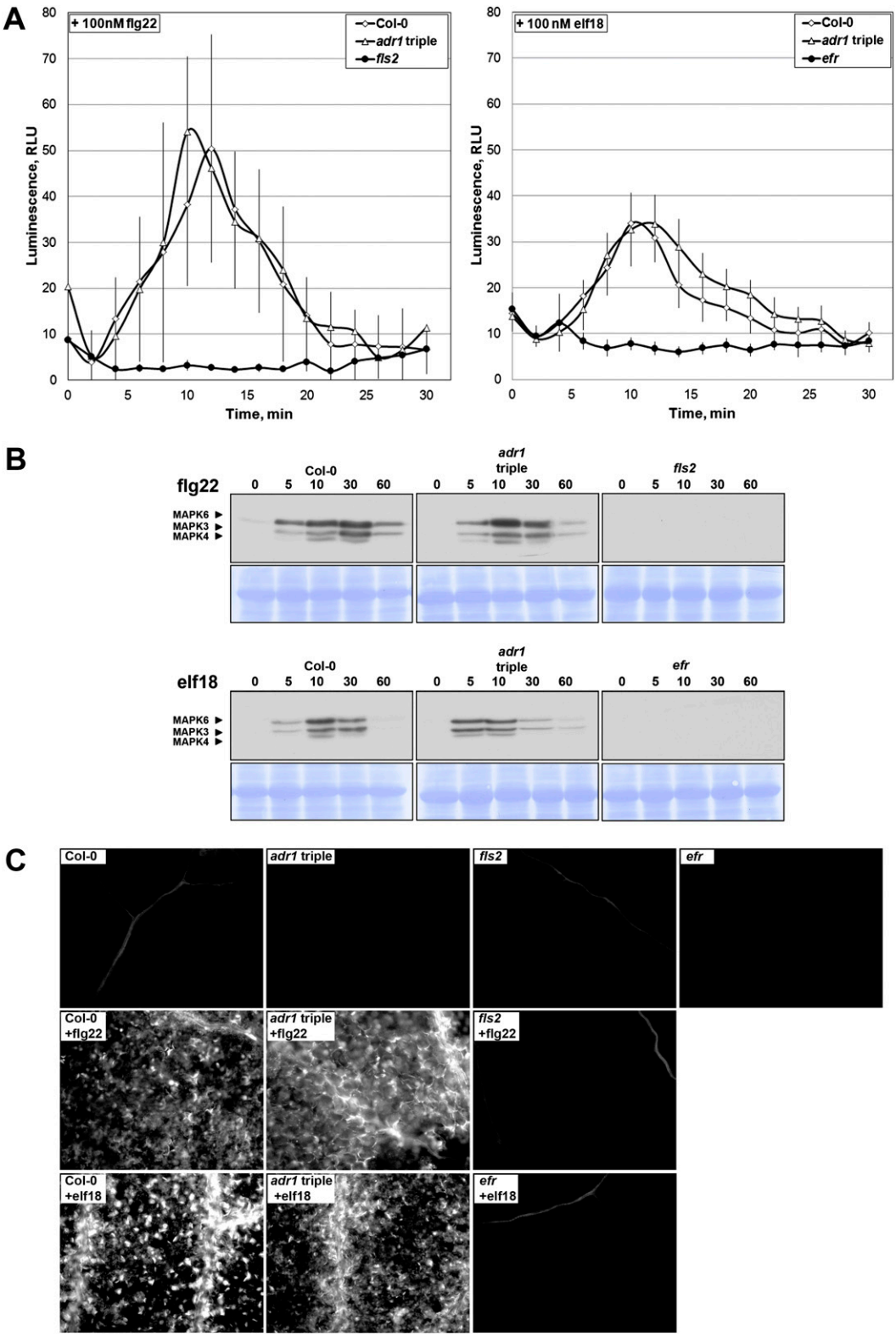

Fig. S6. Early responses to flg22 and elf18 do not require the ADR1 proteins. (*A*) Oxidative burst in leaves of the indicated genotypes after addition of 100 nM flg22 (*Left*) or elf18 (*Right*). Results are means ± 2 × SE ($n = 8$). (*B*) MAPK activation in seedlings of the indicated genotypes upon application of 1 μM of flg22 or elf18 over time. The identity of each band is shown on the left. Equal loading was verified by Coomassie stain. (*C*) Callose deposits stained with aniline blue on the cotyledons of seedlings treated with water (*Top* panels), 1 μM flg22 (*Middle* panels), or 2 μM elf18 (*Bottom* panels) for 24 h. Images are representative of 20 individuals.

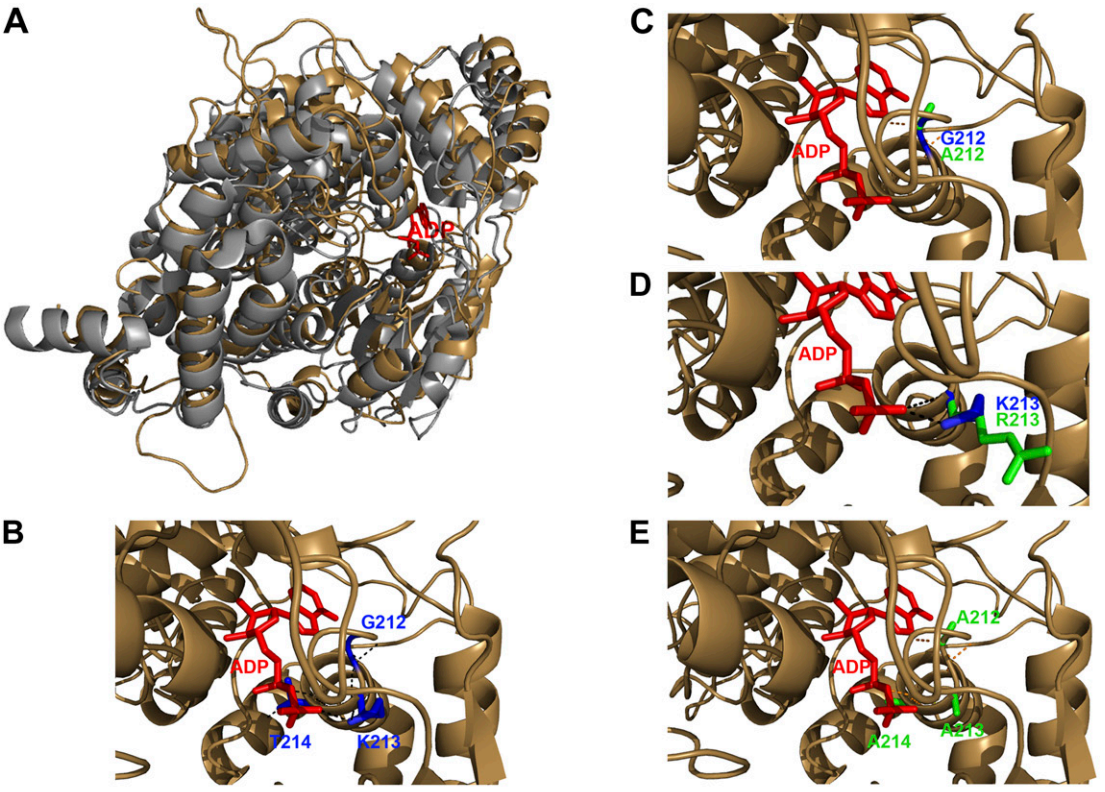

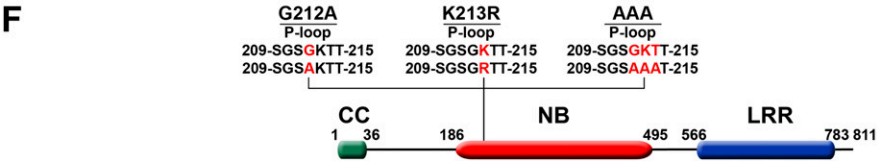

G

Organism	Protein	Architecture	P-loop	Mutation
Arabidopsis thaliana	ADR1-L2	CC-NB-LRR	207-gmsgsg**k**ttlake-219	G212A
Arabidopsis thaliana	RPM1 (27)	CC-NB-LRR	200-gmggsg**k**ttlsan-212	G205E
Homo sapiens	pUL56 (28)	ATPase	709-ynetfg**k**qlsiac-721	G714A
Mus musculus	RAD51D (29)	ATPase	107-ggpcsg**k**tqvclc-119	G112A
Homo sapiens	NALP3 (30)	PYD-NB-LRR	226-gaagig**k**ttilark-238	GKT231/232/233AAA
Homo sapiens	NALP12 (31)	PYD-NB-LRR	217-gaagig**k**smlahk-229	GKT222/223/224AAA
Solanum tuberosum	Rx (32)	CC-NB-LRR	170-gmggig**k**ttlatk-182	GK175/176AA
Homo sapiens	NOD1 (33)	CARD-NB-LRR	202-gdagvg**k**smllqr-214	K208R
Homo sapiens	NALP1 (34)	PYD-NB-LRR-CARD	334-gaagig**k**stlarq-346	K340M
Homo sapiens	Apaf-1 (26)	CARD-NB-WD40	154-gmagcg**k**svlaae-166	K160R
Lycopersicon esculentum	I-2 (35)	CC-NB-LRR	201-gmggqg**k**ttlaka-213	K207R
Lycopersicon esculentum	NRC1 (36)	CC-NB-LRR	185-gmpglg**k**ttlatk-197	K191R
Nicotiana tabacum	N (37)	TIR-NB-LRR	216-gmggvg**k**ttiara-228	K222E/N
Arabidopsis thaliana	RPS2 (38)	CC-NB-LRR	182-gpggvg**k**ttlmqs-194	K188L
Arabidopsis thaliana	RPS5 (39)	CC-NB-LRR	183-gmggvg**k**ttlltk-195	K189N
Linum usitatissimum	L6 (40)	TIR-NB-LRR	265-gmggig**k**ttlaka-277	K271M
Caenorhabditis elegans	CED4 (41-43)	CARD-NB-HD1-WHD-HD2	159-gragsg**k**sviasq-171	K165R
Mus musculus	RAD51D (29)	ATPase	107-ggpcsg**k**tqvclc-119	K113R/A
Mus musculus	APS (44)	APS kinase-ATP sulfurylase	59-glsgag**k**ttvsma-71	K65R
Saccharomyces cerevisiae	Vps4p (45)	ATPase	173-gppgtg**k**sylaka-185	K179A
Agrobacterium tumefaciens	VirB11 (46)	ATPase	169-gptgsg**k**ttmskt-181	K175A/R
Erwinia chrysanthemi	PrtD (47)	ATPase	364-gasgsg**k**stlarl-376	K370R
Arabidopsis thaliana	ADR1-L2	CC-NB-LRR	207-gmsgsg**k**ttlake-219	K213R
Arabidopsis thaliana	ADR1-L2	CC-NB-LRR	207-gmsgsg**k**ttlake-219	GKT212/213/214AAA
	Consensus		g**x**xxx**gks/t**	

Fig. S7. ADR1-L2 is structurally similar to Apaf-1. (*A*) Homology model of the CC_R-NB domain (residues 40–671) of ADR1-L2 (brown) based on the crystal structure of ADP-bound Apaf-1 (26) (gray). (*B*) The location of the conserved functionally relevant G212, K213, and T214 of ADR1-L2 is illustrated in blue inside the ADP-binding pocket. (*C*) Model of the structural reorganization caused by the substitution of G212A in ADR1-L2. G212 maps to the Apaf-1 G159 and forms a polar contact (orange dashed line) to a neighboring residue in the polypeptide backbone. A mutated ADR1-$L2_{G212A}$ (green) forms an additional contact (dark brown dashed line) with another neighboring residue, which is likely to result in a different secondary structure or in the elongation of the α-helix. (*D*) Model of the structural reorganization caused by the substitution of K213 in ADR1-L2. K213 maps to the Apaf-1 K160, and in both cases the Lys residue is predicted to coordinate ADP via two hydrogen bonds (dashed lines). A mutated ADR1-$L2_{K213R}$ (green) loses the coordination of ADP. (*E*) Model of the structural re-

Legend continued on following page

organization caused by the substitution of GKT212/213/214AAA in ADR1-L2. (*F*) Schematic representation of ADR1-L2 showing the P-loop mutations described in this study. The amino acid changes are shown in relation to their linear position. The CC domain is shown in green, the NB domain in red, and the C-terminal LRR domain in blue. (*G*) Alignment of the P-loop domain from various plant, animal, and bacterial STAND proteins and ATPases for which mutations in this motif result in loss of function. The consensus sequence is displayed on the bottom. Residues highlighted in red represent essential amino acids required for the coordination of ATP/ADP and their mutations (substitutions are shown on the right) resulted in loss-of-function proteins [references are listed in parentheses in the protein column (27–47)]. Green indicates that the mutation does not cause loss of function.

Correction

PLANT BIOLOGY

Correction for "Expanded functions for a family of plant intracellular immune receptors beyond specific recognition of pathogen effectors," by Vera Bonardi, Saijun Tang, Anna Stallmann, Melinda Roberts, Karen Cherkis, and Jeffery L. Dangl, which appeared in issue 39, September 27, 2011, of *Proc Natl Acad Sci USA* (108:16463–16468; first published September 12, 2011; 10.1073/pnas.1113726108).

The authors note that Fig. 2 appeared incorrectly. The corrected figure and its legend appear below.

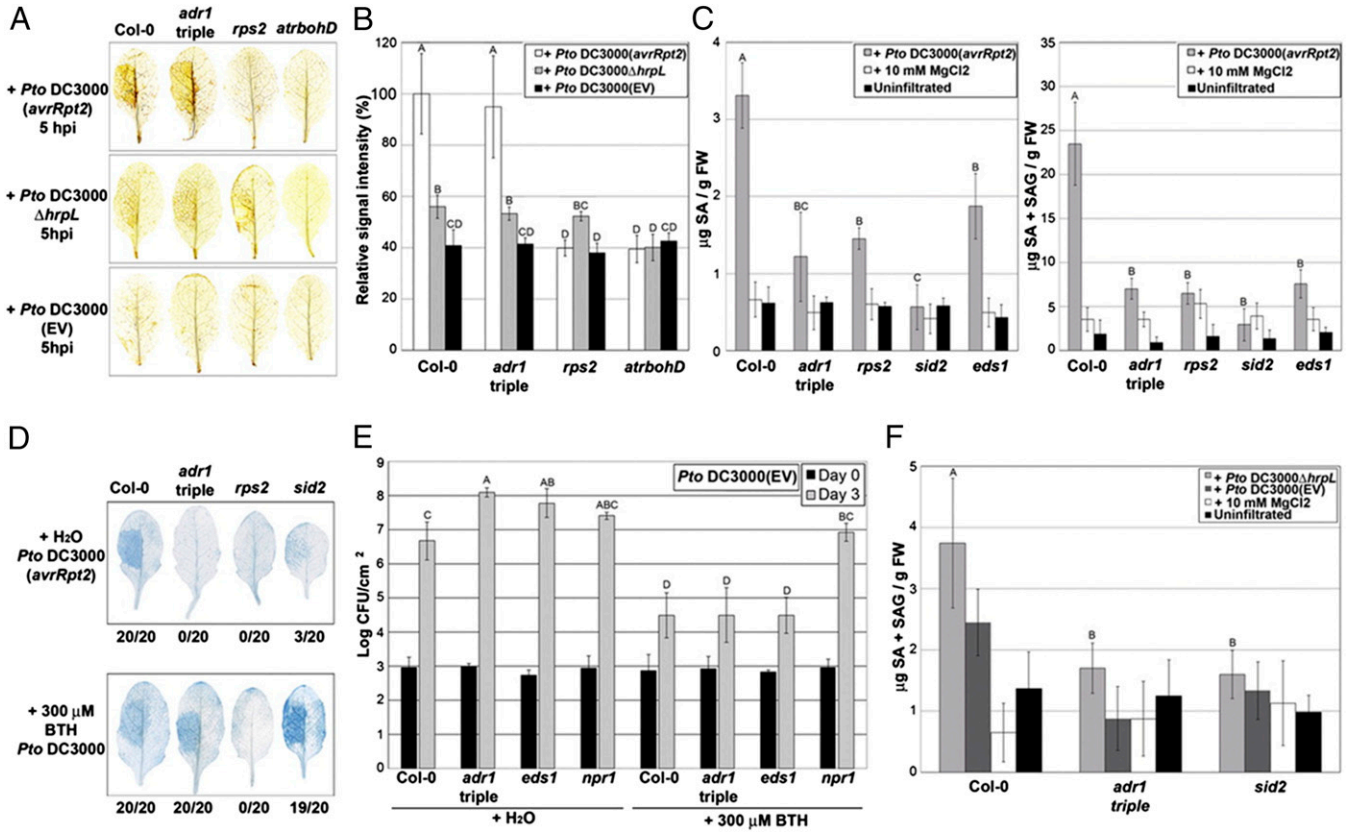

Fig. 2. ADR1 proteins are required for effector-independent SA accumulation following a superoxide burst. (*A*) Leaves from 4-wk-old plants were hand-infiltrated with *Pto* DC3000(*avrRpt2*), *Pto* DC3000Δ*hrpL*, or *Pto* DC3000(EV). H_2O_2 accumulation was monitored by 3′,3′-diaminobenzidine (DAB) staining at 5 h post inoculation (hpi). Leaves are representative of 10 individuals. (*B*) DAB staining shown in *A* was quantified (mean ± 2 × SE, $n = 5$). Letters indicate a significant difference following post-ANOVA Student's *t* test ($\alpha = 0.05$). (*C*) Leaves from 4-wk-old plants were hand-infiltrated with *Pto* DC3000(*avrRpt2*) or with $MgCl_2$. Free (*Left*) and total SA (*Right*) were measured at 24 hpi (mean ± 2 × SE, $n = 4$). (*D*) *Pto* DC3000(*avrRpt2*) was hand-infiltrated into leaves from 4-wk-old plants pretreated with either H_2O (*Upper*) or BTH (*Lower*) 24 h before bacterial infiltration. Leaves were collected 10 hpi and stained with trypan blue. Leaves are representative of 20 individuals. Numbers indicate how many leaves showed HR out of the total number of leaves analyzed. (*E*) Four-week-old plants were sprayed with either H_2O or BTH. Leaves were hand-infiltrated with *Pto* DC3000(EV) 2 d post application (dpa). Bacterial growth was monitored at 0 and 3 dpi, mean ± 2 × SE ($n = 4$). (*F*) Leaves from 4-wk-old plants were hand-infiltrated with *Pto* DC3000Δ*hrpL*, *Pto* DC3000(EV), or $MgCl_2$. Total SA was measured at 9 hpi (mean ± 2 × SE, $n = 4$) and compared with SA levels from uninfiltrated plants. Letters indicate a significant difference among genotypes infiltrated with *Pto* DC3000Δ*hrpL* following post-ANOVA Student's *t* test ($\alpha = 0.05$). The experiments in *A*–*F* were repeated three times with similar results.

www.pnas.org/cgi/doi/10.1073/pnas.1620070114